Project Progress Final Report

Low Cost PEM Fuel Cell Metal Bipolar Plates

Award Number*:*

DE-EE0000463

TreadStone Technologies, Inc.

Performance Period: Oct. 1, 2009 – Feb. 28, 2013

Primary Investigator: Conghua "CH" Wang

Team Partners:

Ford Motor Company

Gas Technology Institute

Oak Ridge National Laboratory

Stony Brook University

IBIS Associates, Inc.

May 30, 2013

Executive Summary

Bipolar plate is an important component in fuel cell stacks and accounts for more than 75% of stack weight and volume. The technology development of metal bipolar plates can effectively reduce the fuel cells stack weight and volume over 50%. The challenge is metal plate corrosion protection at low cost for broad commercial applications.

This project aimed to develop innovative technological solutions to overcome the corrosion barrier of low cost metal plates. Its feasibility has been demonstrated and patented (US Patent 7,309,540). The plan is to further reduce the cost and scale up the technology. The project is built on three pillars: 1) robust experimental evidence demonstrating the feasibility of TreadStone technology, 2) a team that consists of industrial leaders in fuel cell stack application, design, and manufacture; and 3) a low-risk, significant-milestone driven program that proves the feasibility of meeting program objectives

The implementation of this project will reduce the fuel cell stack metal bipolar separator plate cost which accounts for 15-21% of the overall stack cost. It will contribute to the market adoption of fuel cell technologies. In addition, this corrosion protection technology can be used similar energy devices, such as batteries and electrolyzers. Therefore, the success of the project will benefit in a broad markets spectrum.

1. Project Objectives and Scope

The objective of the project was to develop low cost Polymer Electrolyte Membrane (PEM) fuel cell metal bipolar plates using TreadStone's proprietary technologies. The project also sought to demonstrate the performance, including the long-term operation stability of the low-cost metal bipolar plate for portable, stationary and transportation operating conditions.

The project is based on TreadStone's patented low-cost PEM fuel cell metal bipolar plate technology that currently uses stainless steel (SS) as the substrate material. The focus of the project is to further reduce the metal bipolar plate cost by using carbon-Steel, Aluminum and other low-cost materials to meet DOE's 2015 performance and cost targets. We have the innovative solutions to overcome all technical barriers and assembled an qualified team to execute the working plan and mitigate the development risks.

The bipolar plate is an important component in fuel cell stacks and accounts for more than 75% of stack weight and volume. Current technologies use graphite-based bipolar plates in fuel cell stacks. Graphite-based plates are thick and heavy, which considerably increases stack weight/volume, and reduces stack power density. Metal bipolar plate, using thin metal foil, can effective reduce the stack weight and volume. However, due to the aggressive corrosion of metal in fuel cell stacks, metal bipolar plates have not been widely used in PEM fuel cells. In addition, metal bipolar plates have to have low electrical contact resistance and cost for automobile fuel cell applications. This project is aimed to overcome these technical barriers by the innovative technology development.

Through this project we have achieved the planned goals and objectives.

1. Developed lower cost conductive dots materials and processing technology to minimize or eliminate gold usage in the bipolar plates.
2. Demonstrated the feasibility of using low cost carbon steel and aluminum as the bipolar plate substrate materials.
3. Completed the fabrication cost analysis. It was found that TreadStone's metal plate technology can meet the 2015 cost target defined by DOE.
4. Demonstrated the application of TreadStone's metal bipolar plate technology in PEM fuel cell stack applications. Most significantly, the technology has demonstrated the stable operation in automobile fuel cell stacks under the dynamic operation condition at Ford.

The success of this project has led to the commercial adoption of this technology in PEM fuel cells and electrolyzer markets.

2. Project Progress

The project includes three major technical tasks to develop the low cost conductive vias (dots) materials, substrate materials and the demonstration of the low cost metal plates in PEM fuel cell stacks. The activities of each task are summarized in following sections.

Task 1 Conductive Via Processing Development

The objective of this task was to reduce or eliminate gold (Au) in TreadStone's current technology. The candidate conductive vias (dots) materials investigated in this task include palladium, carbon nanotubes, and electrically conductive metallic carbides. The optimization and the scale up of TreadStone metal plate production process was also performed in this task. The baseline substrate material for this development was focused on commercial available 316L stainless steel.

- *Palladium Conductive Dots*

As a precious metal, Palladium (Pd) has excellent corrosion resistance in PEM fuel cell application conditions. Its cost is about 1/3 of gold, which has the potential to reduce the meal plate cost. However, it was found that Pd was still subject to the oxidization in fuel cell operation condition because its electrochemical potential (0.951 V_{NHE}) is not high enough for the transit high potential spikes during stack start-up and shut-down process. It was found that surface contact resistance of metal plates with Pd increased after high potential (1.0 V_{NHE}) polarization tests, due to the formation of non-electrically conductive palladium oxide on the surface. Therefore, a small amount of gold is still needed to maintain the low electrical contact resistance of the metal plate.

The process we have developed is to use TreadStone's proprietary thermal spray process to deposit Pd particles on the SS substrate in the form of Pd splats, then to electroless plate Au on the Pd splat surface. Figure 1 shows the SEM picture of a Pd splat with gold on the surface. Gold was deposited in the form of small particles (light gray particles in the picture) covering a portion of the Pd surface. The thickness of the gold particle was ~40 nm.

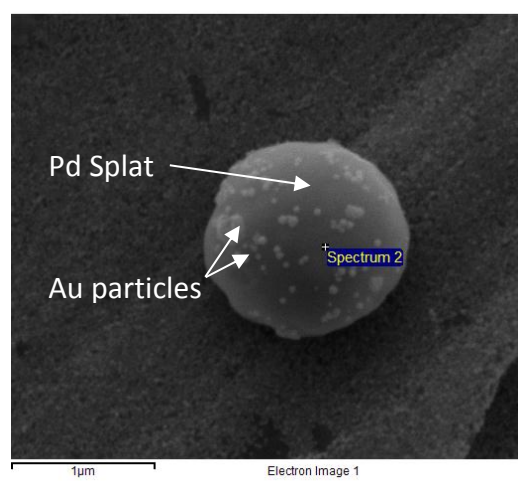

Figure 1. SEM picture of a Pd splat with Au particles on the surface.

On the standard thermal sprayed plates, the small Pd splats covered 1-3% of the SS substrate surface. The gold was then plated on the Pd splats surface. The electrical contact resistances of the plates were measured with the SGL 24 BA Gas Diffusion Layer (GDL) under ~150 psi compression

pressure and 1 A/cm^2 current density. It was found that the contact resistance was related to the coverage of Pd splats on the substrate surface. As shown in Table 1, with 1-3% area coverage of Pd on SS surface, the contact resistance was between 2-12 mΩ.cm^2.

The corrosion tests were conducted in pH2 H_2SO_4 + 5 ppm HF solutions under 1.0 V_{NHE} of polarization potential at 80°C. This test condition was more aggressive than the standard corrosion test condition DOE recommended (under ~0.8V_{NHE} corrosion potential). The corrosion current of the SS plates with Pd/Au splats was below 1 μA/cm^2. The comparison of electrical contact resistance before and after the corrosion test is shown in Table 1. It shows that contact resistance of the metal plates with Pd/Au splats did not increase after the corrosion test, which met the corrosion resistance requirement

***Table 1. Comparison of the Electrical Contact Resistance of GDL with SS/Pd Plates before and after the Corrosion test under* 1.0 V_{NHE} in pH2 H_2SO_4 + 5 ppm HF Solution at 80°C**

Sample #	Electrical Contact Resistance (mΩ.cm^2)	
	Before Test	After 100 hrs Test
#1	2	2
#2	10	6
#3	11	12
#4	5	4

- *Carbon Nanotubes*

Carbon nanotubes have been identified as the candidate conductive dots material because of its excellent corrosion resistance with its highly crystallized structure, and its superior electrical conductance. It has the potential to eliminate gold usage on metal plates.

A chemical vapor deposition (CVD) process has been used to grow carbon nanotubes on the surface of stainless steel plates. Various reaction parameters (including precursors, temperature, reaction time, substrate pretreatment conditions, etc.) have been investigated for carbon deposition on SS substrates. It was found that the carbon could be deposited on SS with various crystal structures, from amorphous structure to carbon nanotubes. The deposited carbon crystal structure was highly related with the precursor and the processing temperature. It was found that the lower processing temperature would lead to more amorphous carbon deposition, which is not stable in fuel cell operation conditions. On the other hand, higher processing temperature would result in the better crystallized carbon on the substrate. But, there are higher risks of the reaction between carbon and SS substrate at high temperature, to form carbides (stainless steel sensitization) on the surface and lead to the poor corrosion resistance of the metal plates. It was found that it was critical to control the process conditions (processing temperature and metal plate pre-treatment conditions) to avoid the sensitization.

In this project, we have identified a stainless steel surface treatment process to prevent the stainless steel sensitization. With this treatment process, the CVD processing temperature could be as high as 900°C, which was sufficient to grow well crystallized carbon tubes.

We have used the process to deposit carbon on SS substrate to meet the electrical and corrosion resistant requirements for fuel cell applications. Figure 2 shows a SEM picture (left) of carbon nanotube deposited on SS substrate, and the corrosion current (right) of the SS plate with carbon nanotubes under $0.8V_{NHE}$ polarization potential in pH3 H_2SO_4 + 0.1ppm HF solution at 80°C. The corrosion current was less than 0.1 $\mu A/cm^2$ and keeps going down with time. The electrical contact resistances were well below $10m\Omega.cm^2$ with SGL 24BA GDL under the compression pressure of ~150 psi, as summarized in Table 2.

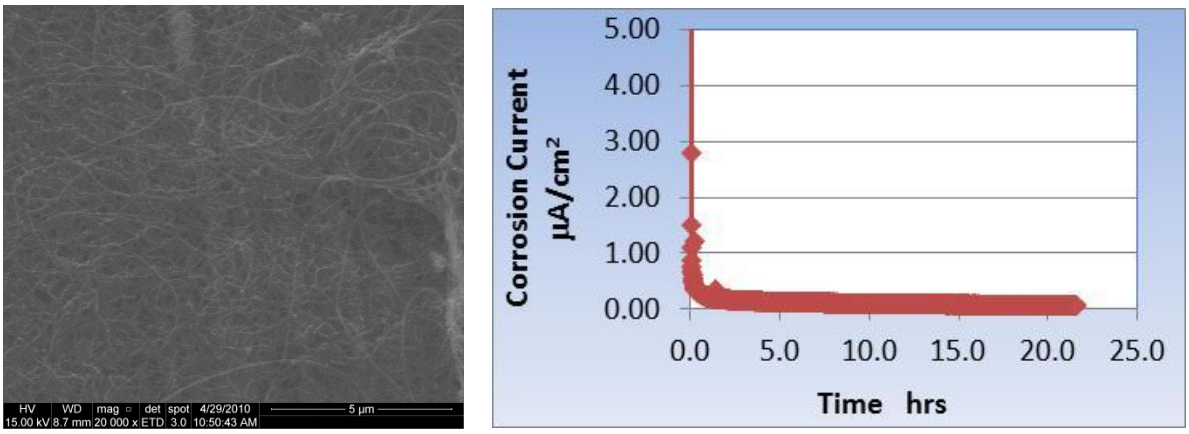

Figure 2. SEM picture of carbon nanotubes deposited on SS by CVD process and the potentiostat corrosion current under $0.8V_{NHE}$ polarization in pH3 H_2SO_4 + 0.1ppm HF solution at 80°C .

Table 2. The Electrical Contact Resistance of GDL with SS w/ Carbon Nanotubes before and after the Corrosion test under 0.8 **V_{NHE} in pH3 H_2SO_4 + 0.1 ppm HF Solution at 80°C**

Sample #	Electrical Contact Resistance ($m\Omega.cm^2$)		
	Before Test	After 20 hrs Test	After 100 hrs Test
SS w/ C	2	0.5	7

However, it was found that stainless steel plates with carbon nanotubes did not have desired corrosion resistance at higher potential. After long term (100 hours) corrosion tests under $1.0V_{NHE}$, the adhesion of carbon nanotube on the SS substrate was reduced significantly. It could be easily wiped off the plate surface after the $1.0V_{NHE}$ test. The hypothesis is that there were some catalyst for the carbon nanotube growth (typically iron or nickel) still on the carbon/SS interface. The catalyst material could be dissolved in severe corrosion conditions

which led to the loss of the adhesion of carbon tube on the metal plate surface. Therefore, this material can only be used in fuel cell stacks operated under mild conditions, without transit high voltage spikes, through proper system control.

- *Metallic Carbide Dots*

It was reported that some carbides have good corrosion resistance in PEM fuel cell conditions. The material cost of these carbides is acceptable. The key issue is the cost processing techniques for the metal bipolar plate production, which is the focus of this task. This approach could eliminate the gold usage on metal plates.

The thermal spray process for conductive carbides deposition on SS foil has been used in this project. The spray condition has been optimized to have the desired adhesion of splats on stainless steel foil substrate without the damage of the thin foil under the extreme heat of thermal spray process. In typical thermal spray processes, the substrate surface has to be roughed (such as cleaned by sand blast) to increase the bonding area for the sprayed material. However, it is impossible to do this on metal foils, without the distortion of the foil. Because of this limitation, it was found that it is difficult to obtain the good adhesion of pure carbide particles on stainless steel foil surfaces. Therefore, the blended carbides powders, with bonding alloy with the carbides were used for the project. The alloy could be melted in thermal spray processes and then the carbides could be "welded" on the stainless steel foil surface.

Figure 3 shows the microscopy picture of the Cr_3C_2-NiCr splats in the SS surface. The optical microscopy picture (A) shows that Cr_3C_2-NiCr particles are randomly and uniformly distributed on the substrate surface. The blended powder has the particle size of 20-50 μm. The finished SS surface is fairly rough because of the large carbide bumps (~ 40 μm). SEM picture (B) shows that the NiCr alloy component in the power was bonded (welded) Cr_3C_2 particles on SS substrate. The smooth surface of the Cr_3C_2 particle indicates that NiCr alloy remains on the top of the carbide surface in the form of a thin cover, which can be removed by a post spray etching step to fully expose the Cr_3C_2 surface for electrical contact with GDL.

The electrical contact resistance of the sprayed SS with GDL was between 15-20 $m\Omega.cm^2$. The carbide type (Cr_3C_2 or WC) and loading on the surface did not make a major difference in contact resistance. However, it was found that the contact resistances were reduced to 5-8 $m\Omega.cm^2$ after cathodic corrosion at $1V_{NHE}$ in acid solutions. In contrast, it was found that stainless steel had a significant increase of the contact resistance under same corrosion condition. Therefore, the reduction in contact resistance of the SS with carbide splats was definitely the contribution from carbides, instead of SS substrate and the bonding alloy. The hypothesis is that the carbide was slightly oxidized during thermal spray, left a thin oxide layer on the surface. The corrosion at $1V_{NHE}$ removed the oxide layer and exposed the conductive carbide surface that led to the lower contact resistance.

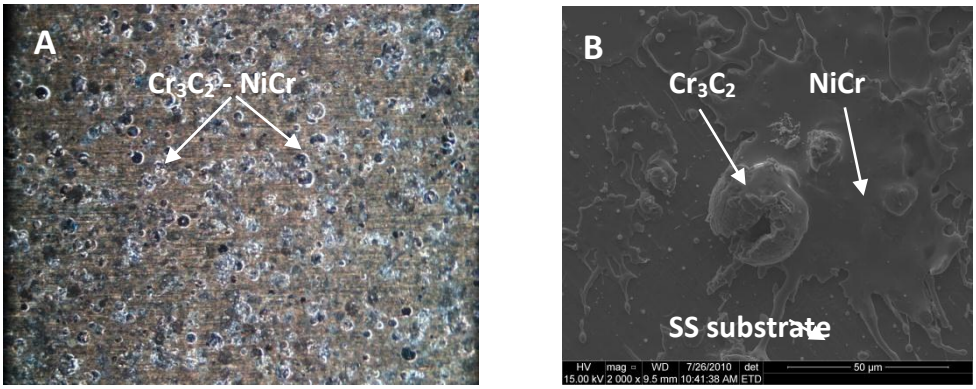

Figure 3. Optical microscopy (A) and SEM (B) pictures of Cr_3C_2 particles bonded on SS substrate by NiCr alloy

It was also found that the corrosion current of the as sprayed WC-CoCr on SS had the highest corrosion current among Cr_3C_2-NiCr coated SS, WC-CoCr coated SS, and bare 304 SS. Bare 304 has lowest corrosion current. Figure 4 shows that the cathodic corrosion current is about 0.9μA/cm^2 for Cr_3C_2-NiCr coated SS after 4 hours corrosion and keep going down, but ~80 μA/cm^2 for WC-CoCr coated SS in pH3 H_2SO_4 + 0.1ppm HF under 0.8V_{NHE} at 80°C. Microscopy observation found that there were some corrosion marks on NiCr alloy portion of Cr_3C_2-NiCr splats, but no corrosion mark on CoCr alloy portion of WC-CoCr splats. WC particles changed color to slight green in some corrosion tests. It is assumed that the as sprayed NiCr and CoCr (with 20-25% Cr) alloys were in amorphous phase and did not have good quality Cr rich surface oxide scale to protect metal from corrosion, like 304 SS or 316 SS, which leads to the higher corrosion current of Cr_3C_2-NiCr coated SS than that of bare SS. WC might not have the desired corrosion resistance, which was the reason of the very high corrosion current of WC-CoCr on SS.

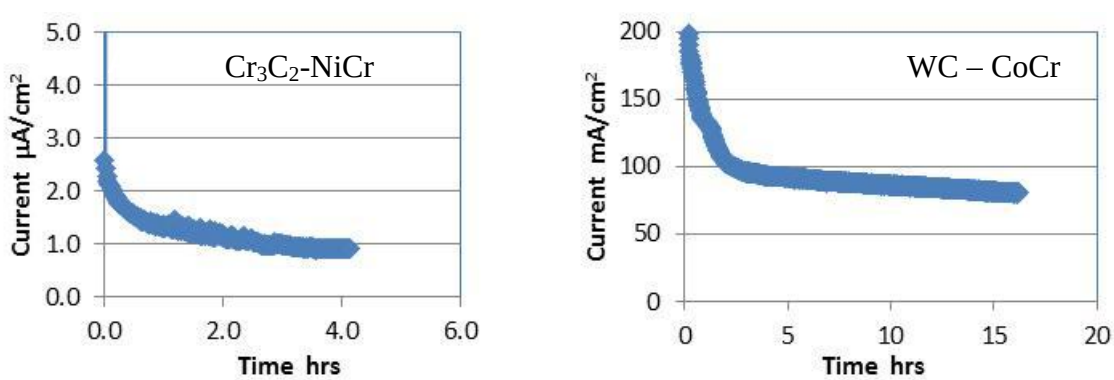

Figure 4. Potentiostat corrosion current of SS foil with Cr_3C_2-NiCr or WC – CoCr splats in pH3 H_2SO_4 + 0.1ppm HF under 0.8V_{NHE} at 80°C.

Figure 4 shows that the corrosion current of the thermal sprayed the common Cr_3C_2-NiCr ($Ni_{80}Cr_{20}$) alloyed powder can meet DOE's corrosion resistant requirement (<1 $\mu A/cm^2$) at the standard testing condition ($0.8V_{NHE}$ in pH3 H_2SO_4 + 0.1ppm HF), although it is higher than that of bare 304SS and 316SS. In order to identify the reason of the higher corrosion current, we examined the corrosion behavior of Cr_3C_2 and $Ni_{80}Cr_{20}$ alloy powders separately. It was found that the $Ni_{80}Cr_{20}$ had relative high corrosion current, and Cr_3C_2 is more stable in the cathodic corrosion condition. The same corrosion experiments were conducted with pure Cr coated SS and found that stainless steel with a pure chromium coating had lower corrosion current than that the bare stainless steel. Therefore, it is possible to further reduce the corrosion current by using higher Cr content alloy as the binding alloy for carbide particles.

In order to prove this hypothesis, a special formulate Cr_3C_2-Ni_1Cr_{15} power was made by Global Tungsten Powders Corp (GTP). The power was sprayed by air plasma spray on stainless steel foil. Figure 5 shows the SEM picture of Cr_3C_2-Ni_1Cr_{15} splats of the finished plate. The Cr_3C_2 particles were smaller than that in the commercially purchased Cr_3C_2-$Ni_{80}Cr_{20}$ powder. Figure 6 shows the corrosion test data at $0.8V_{NHE}$ in pH3 H_2SO_4 + 0.1 ppm HF solutions at 80°C. The corrosion current of SS with Cr_3C_2-Ni_1Cr_{15} splats was below 0.1 $\mu A/cm^2$, 10x lower than that of SS with Cr_3C_2-$Ni_{80}Cr_{20}$ splats, which indicated that the high Cr content had effectively reduce the corrosion current, and improve the durability of the metal plate in PEM fuel cell stacks.

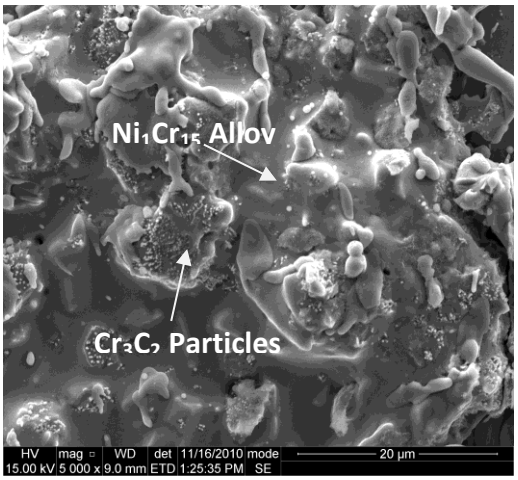

Figure 5. The SEM picture of the ***Cr_3C_2-Ni_1Cr_{15} splats sprayed by air plasma spray***

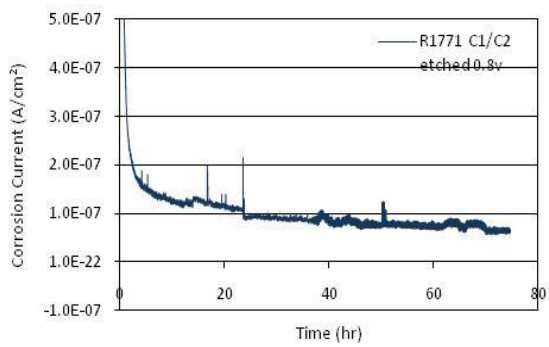

Figure 6. Potentiostat corrosion current of SS with *Cr_3C_2-Ni_1Cr_{15} splats under $0.8V_{NHE}$ in pH3 H_2SO_4 + 0.1 ppm HF solution at 80°C.*

Table 3 shows the electrical contact resistance of GDL with Ni_1Cr_{15} splats coated SS plate, and Cr_3C_2-$Ni_{16}Cr_4$ splats coated SS. The as sprayed plates had high contact resistance, because of the splat surface oxidization during the spray process. The contact resistances were effectively reduced after an electrochemical etching process. Between Ni_1Cr_{15} splats coated SS plate and Cr_3C_2-$Ni_{16}Cr_4$ splats coated SS, the contact resistance of the Cr_3C_2-Ni_1Cr_{15} splats coated plate

had much wider variation. The hypothesis is that the smaller Cr_3C_2 particle size in the Cr_3C_2-Ni_1Cr_{15} splats made it easier to be removed during the etching process. Therefore, the amount of Cr_3C_2 particles on the surface after etching process as the electrical contact points was more difficult to control. It is expected that this problem can be avoided by using larger particle size Cr_3C_2 powder blended with high Cr content alloys.

Table 3. Electrical Contact Resistance of SS with Cr_3C_2-Ni_1Cr_{15} and Cr_3C_2-$Ni_{16}Cr_4$ Splats

Sample #	Contact Resistance mΩ.cm	
	As Received	After Etching
SS w/ Cr_3C_2- Ni_1Cr_{15}	28-62	8-30
SS w/ Cr_3C_2- $Ni_{16}Cr_4$	16-25	5-8

- *Fabrication Cost Analysis*

The fabrication cost analysis of our baseline metal plates using stainless steel and small amount of gold was updated using the recent market materials cost. The analysis was based on the post-forming coating process of stamping and welding the plate before the coating. The schematic drawing and the fabrication process and the assumption of the analysis are shown in Figure 7. It shows that, based on recent SS price ($3.92/lb), the formed and welded 400 cm^2 active area plates cost is $2.06. The coating cost is $0.33/plate, with $0.19/plate of gold material cost. This analysis is based on the plate utilization (active area/plate area) of 50%, which is very conservative comparing with more advanced flow field design. The overall cost of the plate in stacks that have 1W/cm^2 power density is $5.97/kW, with the majority of the cost come from the stainless steel.

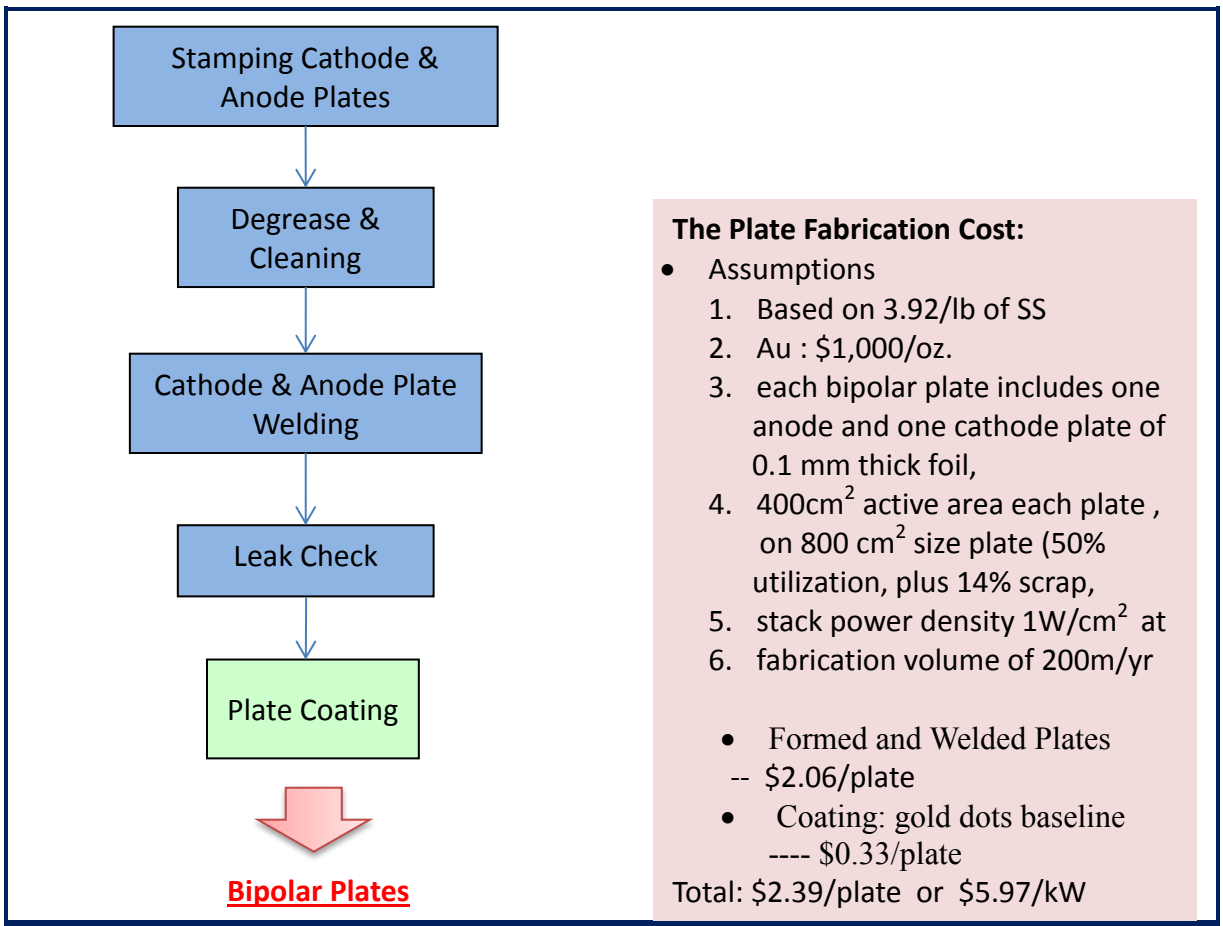

Figure 7. The flow diagram of the plate fabrication process and the assumptions for the plate fabrication cost analysis

Based on the same model, we conducted the cost analysis of the coating cost of the reduced gold, or gold-free approaches developed in this project. The analysis results are summarized in Table 4 and it shows that the new process could reduce the cost. However, the reduction is not as significant as expected because of the additional processing cost of using lower cost materials, and the already low cost ($0.33/plate) of our baseline technology with gold.

The first approach of using Palladium to replace most of gold as the conductive vias is $0.31/plate. Similar as gold, Palladium price has experienced wide fluctuations. Its price has swung between $185/oz and $580/oz in last 5 years. Current price is ~$408/oz. Based on the historical price, the costing could have +/- $0.05/plate fluctuation.

The carbon nanotube approach has the highest cost among all approaches because of the high cost of the chemical vapor deposition process. On the other hand, carbon nanotube may have the risk of the poor corrosion resistance under high voltage condition during the fuel cell shut

down and start up periods. Therefore, it is not worth to further pursue this approach for fuel cell applications.

Among the three processes, the carbide approach is the most promising one. It is a gold-free approach that will avoid the uncertainty of gold price fluctuation. Its cost could be further reduced by eliminate the final chemical etching step with the optimized starting powder properties and the thermal spray process. Carbide as the electrical contacting material has been demonstrated by Honda in their special alloy based metal plates, which demonstrates the feasibility of using carbide for the long term application in PEM fuel cells.

Table 4. The coating production cost analysis of the new conductive vias processing

Process	**Baseline gold dots**	**Pd vias w/ gold**	**Carbon Nanotubes**	**Carbides**
Coating Cost	$0.33/plate	$0.31/plate	$0.79/plate	$0.30/plate

- *Conductive Dots Processing Scale-up and Optimization*

The optimization and scale up of the metal plate production was focused on the thermal spray process to deposit the conductive dots materials. The experiments were mainly carried out using gold as the conductive material.

The initial studies were conducted on the splat morphology observation under various spray conditions, using Scanning White Light Interferometry (Zygo New View 200). Several splats were found, and all splats had thickness less than 2 µm. Figure 8 shows the Zygo images of a large gold splat (~ 10 µm in diameter) on stainless steel sheet. The left image shows the top view and the contour indicates the thickness variation of a splat. The top-right image shows the 3-D view of the large gold splat. From the scale in the top-right image, the splat diameter is ranging from 1-15 µm. Because of the surface roughness of the SS foil, it is difficult to observe the morphology of small splats.

The splat under the red arrow in Figure 8 was denoted by splat-A. The thickness profile was obtained on the center horizontal line, and shown at the right of Figure 8. It was found that the splat was not uniform in thickness. There were two round rims in the splat. The diameters is around ~11 µm, and the thickness variations are from ~1.0 µm at peak, to 0.1 µm at valleys.

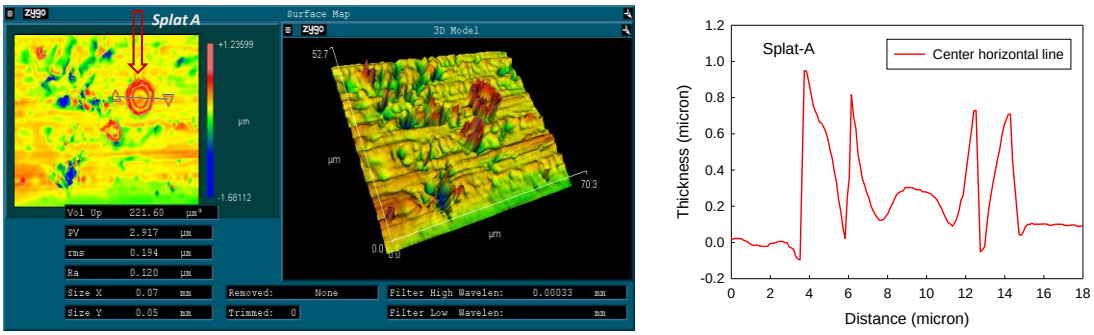

Figure 8. Zygo screen-shot for splat study (left image, top view right image, the 3-D view), and the thickness profile for the center horizontal line of Splat-A

The morphology of small splats was observed on a smooth silicon wafer surface and their microscopy picture is shown in Figure 9. The thickness profiles of splat A and B (~2 µm in diameter) are also shown in Figure 9. It shows that the small gold splats have a more smooth morphology than the larger splat in Figure 8. The peak high (gold thickness at highest spot) is between 0.1 and 0.2 µm.

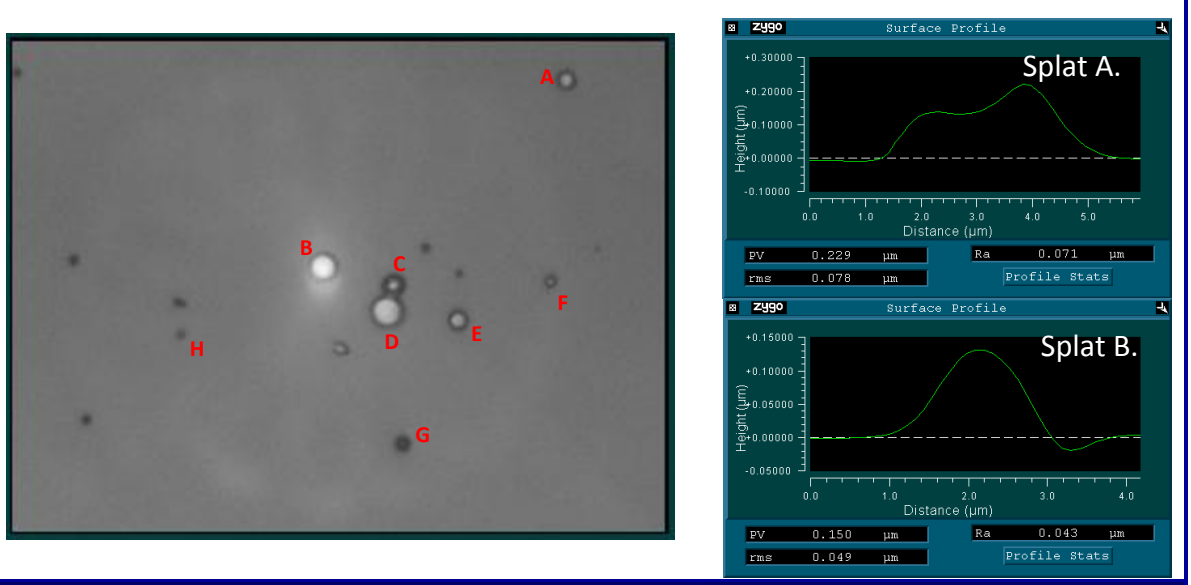

Figure 9. Optical microscopy image of gold splats on Silicon wafer and the thickness profile of splat A and B.

The morphology of gold splats can be controlled by the thermal spray conditions. Figure 10 shows the SEM pictures and the schematic drawings of the gold splats deposited under

different conditions. Figure 10A shows the small spherical shaped splats. It has less bonding strength with the SS substrate. However, it has low electrical contact resistance, presumably due to its high morphology, which makes it easier to stand out the valley of the rough substrate surface for the electrical contact with GDL. On the other hand, the flat splats, as shown in Figure 10B, have better adhesion with substrate due to the lager bonding area between splats and the substrate.

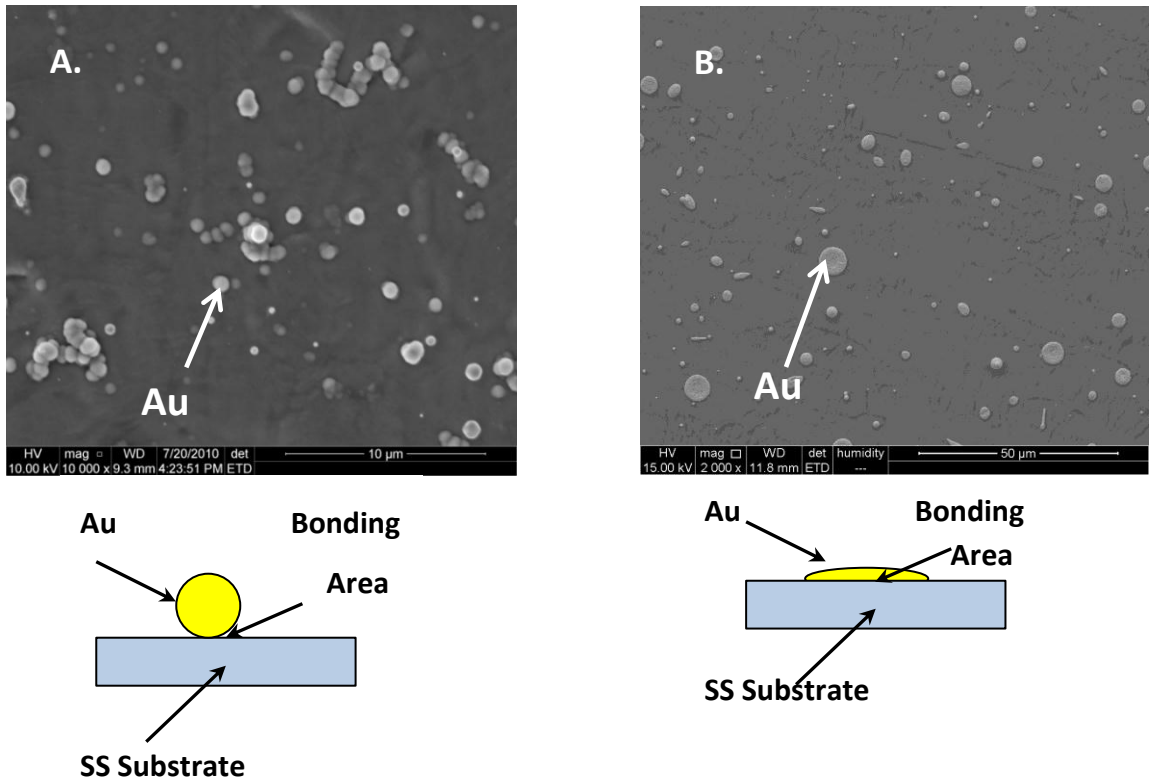

Figure 10: SEM pictures and schematic drawing of gold splat on substrate.

A. spherical gold splats, B. flat gold splats

In this project, we have scaled up the thermal spray system for the full size automobile fuel cell plates production. Figure 11 shows the metal bipolar plates we processed for Ford Motor Company. Table 5 summarizes the through plate voltage (TPV) drop of the plate in contact with GDL at 1A/cm^2 current density with 90 psi compression pressure. The value of this TPV is the same as the through plate resistance (due to 1A/cm^2). The TPV of the plates are very uniform across the plates and between the plates, which meets Ford's requirement. After the process was scaled up, we produced 40 bipolar plates with the optimized process conditions for the durability test of a 20-cell stack at Ford.

Table 5. Through Plate Voltage (TPV) Drop of Ford's Bipolar Plates with TreadStone's Baseline Coating Technology at Different Measurement Points.

Plate #	TPV at 1A/cm^2				
	A	B	C	D	Average
#1	6.75	6.14	6.64	6.45	6.50
#2	5.36	6.25	6.95	6.60	6.29
#3	7.60	7.12	7.00	6.40	7.03
#4	7.00	6.40	6.00	7.40	6.70
#5	7.60	6.90	7.50	7.50	7.38

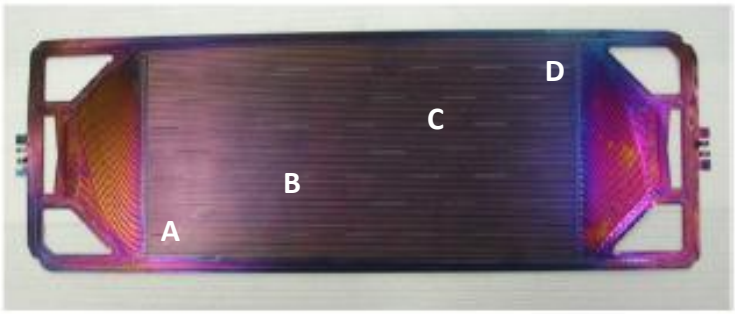

Figure 11. Picture of the full size metal bipolar plate processed with TreadStone's technology. The notation of A, B, C, D indicates the TPV measurement points of Table 5.

Task 2. Carbon Steel and Aluminum Based Plates Development

The objective of this task was to replace the SS substrate in TreadStone's current technology with low-cost Carbon Steel (C-steel) and Aluminum (Al). This task would mainly use Au as the conductive vias material. The impact of the new substrate materials and processing technologies on the performance (corrosion resistance and electrical contact resistance) of metal plates would be evaluated. Failure mode and fabrication cost analysis will also be conducted.

- *C-Steel-Based Metal Plate Developments*

TreadStone's approach for the carbon steel protection is to apply a corrosion resistant (could be non-electrically conductive) material to cover the plate surface, and then apply the gold dots as the electrical conducting pathway for the bipolar plate.

The non-conductive and corrosion resistant materials that have been investigated in this project were Silicon (Si), Silicon carbide (SiC) and Silicon Nitride (Si_3N_4). A thin layer of Si, SiC or Si_3N_4 was applied on carbon steel surface by chemical vapor deposition (CVD) or plasma enhanced CVD (PECVD) process. The Si coating layer was 2-3 µm thick, SiC and Si_3N_4 coating layer was 0.2-0.3 µm thick. The corrosion resistances of all initial coated samples (without gold splats) were excellent. Then, gold splats were thermally sprayed on the plate surface. At last, the plate was heat treated to diffuse gold through Si or Si_3N_4 that will make the Si and Si_3N_4 more semiconductive. The schematic drawing of the plate is shown in Figure 12. The gold splats were in direct contact with the GDL in fuel cells. Electronic current will come from GDL to gold splats, and then go through the semiconductive Si, SiC or Si_3N_4 layer under the gold splats to the C-Steel core layer. Because of the small thickness of the Si, SiC or Si_3N_4 layer, the electrical resistance though the semiconductive thin film layer could be acceptable.

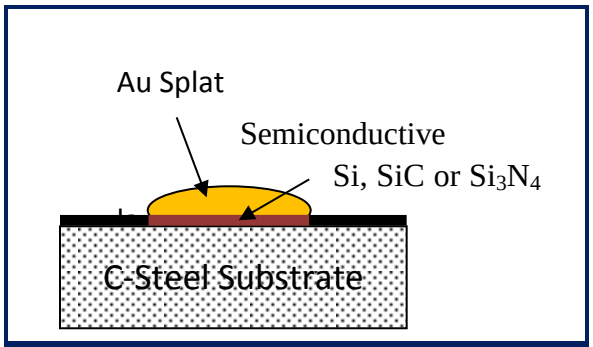

Figure 12. Schematic drawing of Si, SiC or Si_3N_4 coated metal plate with gold splat.

The electrical contact resistance of the coated carbon steel samples through the steps of the process is summarized in Table 6. It was found that the electrical contact resistances of the as sprayed plates were very high. After heat treatment, the resistance of Si coated plates with gold splats was reduced to below 10 $m\Omega/cm^2$. The SiC coated plate resistance was also reduced, but not low enough for PEM fuel cell application (<10 $m\Omega/cm^2$). The SI_3N_4 coated plate did not show reasonable reduction of the resistance.

Table 6. The Electrical Contact Resistance of GDL with Coated C-Steel with Gold Splats

Coating Material	Electrical Contact Resistance (mΩ.cm^2) with SGL 24BA GDL		
	w/o Gold Splats	w/ Gold before Heat Treatment	w/ Gold after Heat Treatment
Si	~800	~800	<10
SiC	2000 – 3000	2000 – 3000	600 - 700
Si_3N_4	2000 – 3000	2000 – 3000	2000 – 3000

The corrosion resistance of the Si coated carbon steel plates with gold splats has been investigated by cathodic polarization experiment in pH2 H_2SO_4 + 50 ppm HF solutions at 80°C under 1.0 V_{NHE} polarization potential. It was found that the corrosion current was very high. Post corrosion inspection found that severe corrosion took place around gold splats, as shown in Figure 13. The hypothesis is that Si forms eutectic structures around gold splats after heat treatment. This Au-Si eutectic phase may not have the desired poor electrochemical corrosion resistance.

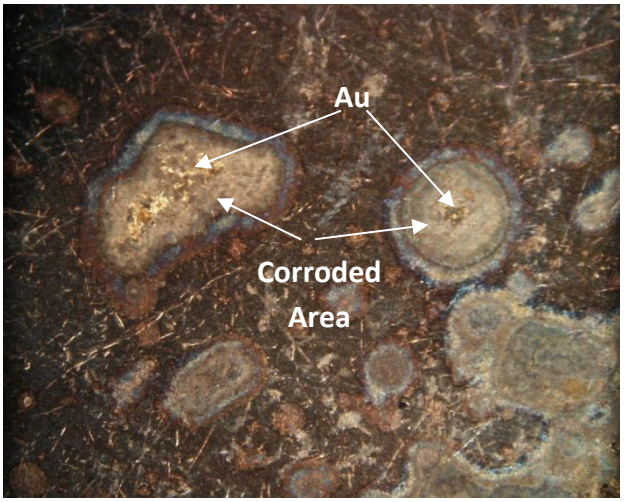

Figure 13. Optical microscopy image of the corroded area around gold particles on Si coated carbon steel

The corrosion tests were also conducted with the SiC coated plates. It was found that, although the SiC coated area had excellent corrosion resistance, it was difficult to avoid coating defects in the thin film coating (0.2-0.3 μm). Consequently, corrosion still took place on these defects.

In order to deal with the coating defects, we used plating process to plate gold through the coating defects on the exposed carbon steel. The hypotheses was to use the gold to plug the defects. The schematic drawing of the structure and the SEM picture of gold plated through the SiC coating layer pin holes are shown in Figure 14 (A & B). The gold plated through the pin-holes was used as the conductive via to keep the low electrode contact resistance of the metal plates with GDL. It was found that the contact resistance of the plate with GDL was <2 mΩ.cm^2.

However, the cathodic corrosion experiments showed that the corrosion current of the SiC coated carbon steel with plated gold vias was still very high, presumably due to small gaps

between the gold vias and the wall of the SiC coating layer. In order to eliminate the gaps, the sample was heat treated at 1000°C. Gold would be better bonded with the carbon steel substrate and the SiC layer by thermal diffusion at this high temperature. However, it was found that the corrosion current actually increased after the heat treatment. SEM picture (Figure 14C) shows that there are a lot of micro-cracks generated on the SiC coating layer after the heat treatment process, which expose more carbon steel. These cracks could be formed due to the thermal expansion coefficient mismatch of the SiC coating layer with that of carbon steel substrate.

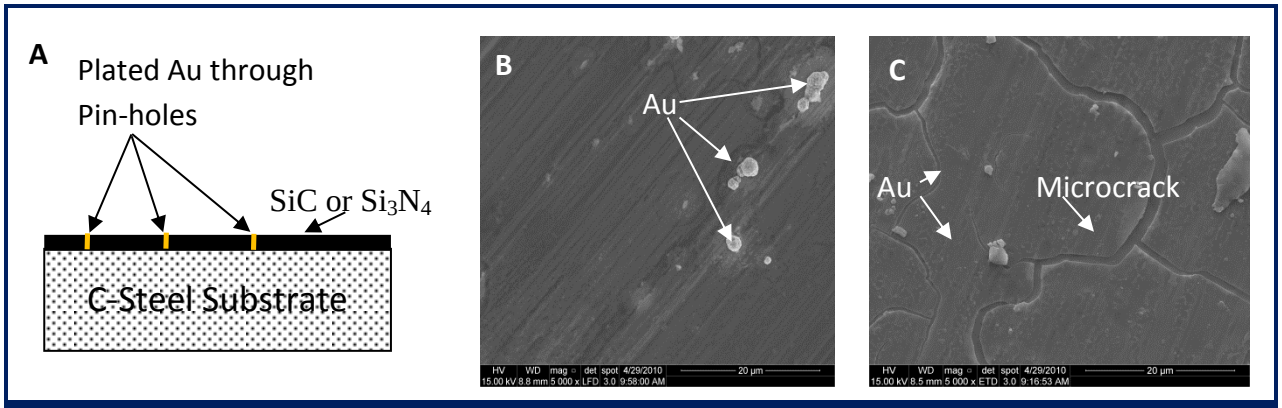

Figure 14. Schematic drawing (A) and SEM picture of as plated gold though the pin-holes of SiC thin film (B) and after 1000°C heat treatment (C)

- *-Aluminum Plate Developments*

The approach to protect Aluminum plates is to deposit a layer of chromium (Cr) using an electrical plating process, then spray gold splats on top of Cr layer to reduce the electrical contact resistance. This was previously demonstrated in the stainless steel plates by TreadStone. The focus of this approach was the selection of the chromium plated aluminum plates.

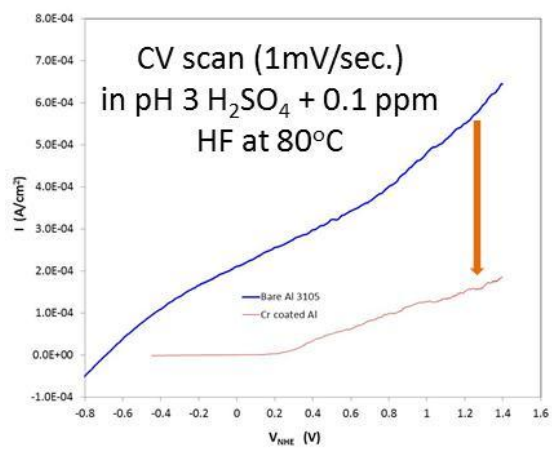

Figure 15. Comparison of CV curves of bare Al 3105 alloy and Cr plated Al alloy plates in pH 3 H2SO4 + 0.1 ppm HF solution at 80°C

The commercial available chromium plated aluminum was first selected for the initial corrosion tests. The cyclic voltammetry (CV) tests of bare 3105 Al and chromium plated aluminum plates are conducted in pH 3 H_2SO_4 + 0.1 ppm HF solutions with the scan rate of 1 mV/sec at 80°C. As shown in Figure 15, plated Cr significantly reduced the corrosion current of Al. At $0.8V_{NHE}$ the corrosion current of bare Al was as high as

400 μA/cm^2, in comparison, that of Cr plated Al is about 70 μA/cm^2. Unfortunately, this corrosion current was still too high for PEM fuel cell applications (need to be < 1 μA/cm^2). Post corrosion inspection found that there was little corrosion marks on most of the Cr plated Al plate surface, except on several spots. SEM/EDAX analysis found that these were high sulfur, oxygen and aluminum content on those corroded spots, but not chromium, as shown in Figure 16. The hypothesis is that these corroded spots were actually exposed aluminum oxide/sulfide inclusions that were not covered by Cr, because Cr could be plated on these nonconductive spots. Therefore, it is important to have the defect free coating, or have the post plating process to cover the plating defects.

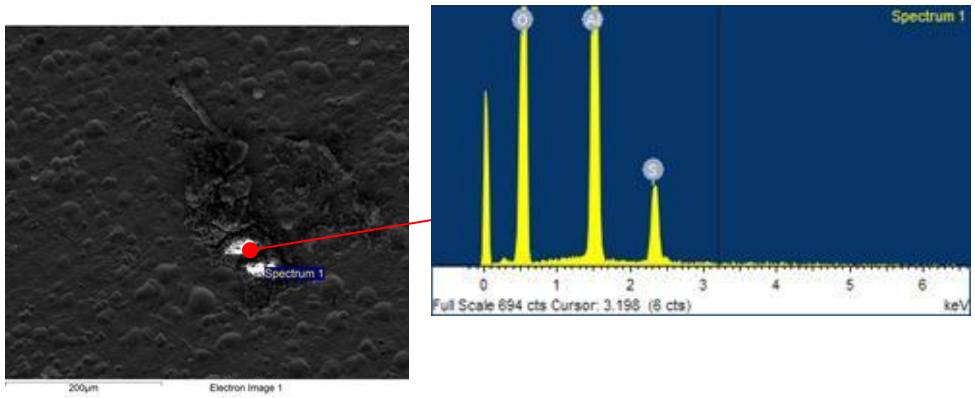

Figure 16. SEM picture of a corroded spot on chromium plate aluminum plate, and the EDAX analysis of the spot

In order to further evaluate the feasibility of using Cr to protect Al plates, we have compared two types of chromium coating on Al. One was the thin Cr (<0.1 μm) on top of a thick Ni interface layer between Cr and Al foil substrate. The other was the thick Cr (2-3 μm) layer on top of a thin Ni interface layer between Cr and Al foil substrate. In order to quickly verify the coating quality, we used an electroless plating process that could plate gold on Ni through the defects of Cr top layer. Figure 17 shows the SEM pictures of thin Cr and thick Cr coated Al plate with the electroless plated Au, indicating the coating defects. It shows that there were a lot of pin holes on the thin Cr coated layer. On the other hand, the thick Cr layer has much less amount of pin holes. Unfortunately, there were some microcracks in the Cr layer. It was found the Cr layer was very hard and could not be conformed to the flexible Al foil. A cracking sound was heard when the Cr plated Al foil was bended, presumably due to the crack of the hard Cr layer. Ideally, a Cr alloy (such as Cr-Ni alloy) is used as the coating layer. It could have similar corrosion resistance as stainless steel, and good ductility to avoid the cracks. Unfortunately, we did not find a plating shop that was capable to provide this type of services.

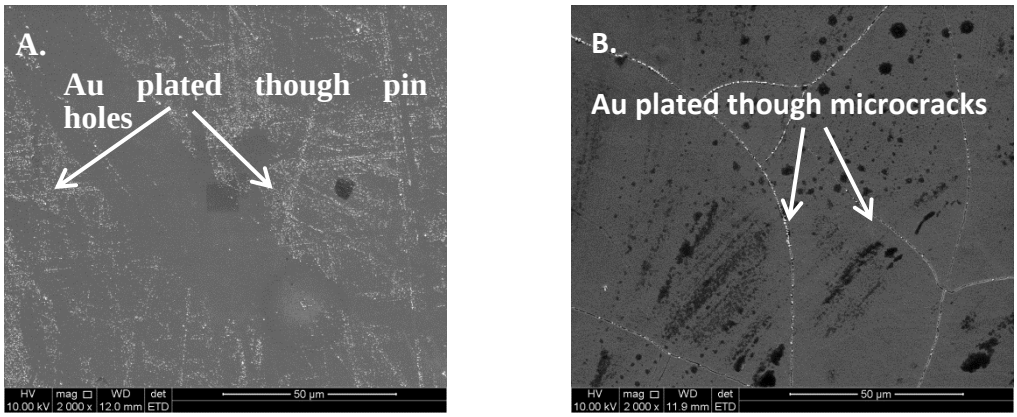

Figure 17. SEM picture of thin Cr (A), and thick Cr (B) coated Al plates with electroless plated gold indicating the coating defects

We did the corrosion tests of the gold plated Cr coated Al plate. The corrosion condition was $0.8V_{NHE}$ in pH3 H_2SO_4 + 0.1 ppm HF at 80°C. The purpose was to evaluate the possibility of using gold to "plug" pin holes of the Cr layer. Figure 18 shows the SEM picture of the corroded Al plates. The corrosion failure of the thin Cr coated Al plate was more significant than the thick Cr coated Al. The thin Cr layer was partially peeled off after the corrosion due to the aggressive corrosion of the Ni interface layer under $0.8V_{NHE}$ cathodic corrosion condition. The thick Cr coated Al still had the corrosion current of >10 $\mu A/cm^2$, although it was smaller than the thin Cr coated Al plate. But it was not low enough for fuel cell applications. The SEM pictures in Figure 18 show the corrosion marks around the pin holes, although they were "plugged" by gold, which means that gold plated through the pin holes was not sufficient to completely prevent the Al plate from corrosion.

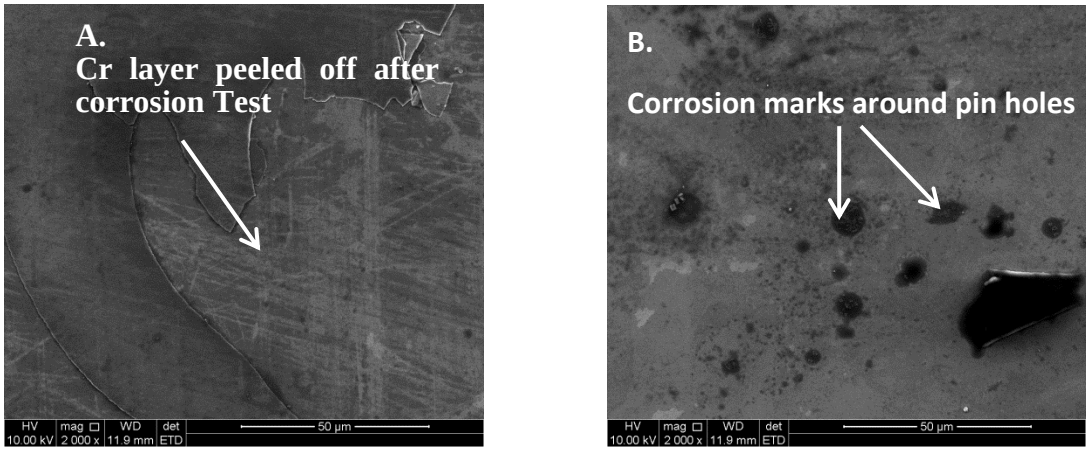

Figure 18. SEM picture of corroded thin Cr (a) and thick Cr (B) coated Al plates

In summary, it is important to have a defect-free coating on carbon steel or Aluminum plate surface to protect the substrate from corrosion because unlike stainless steel, both carbon steel and aluminum have severe corrosion in PEM fuel cell operation conditions, even at low cathodic potential. In addition, there has to be a thorough inspection process of each plate to ensure the "defect-free" coating. This inspection cost will significantly add to the plate production cost. Therefore, the development of the carbon steel and aluminum plate protection technology has to consider these factors in the large volume production. It is possible that the whole plate cost could be higher than stainless steel based bipolar plate, although the substrate material cost of carbon steel and aluminum is much lower.

Task 3 Fuel Cell Stack Application Demonstration (Year 1 & 2)

The objective of this task was to design and demonstrate TreadStone's metal plates in fuel cell stacks for portable, stationary and automobile applications. The target power of portable application stack is 200W, the stationary stack is 2KW, and the automobile stack is 2-5 kW. The focus of this task was on stack performance long-term stability in the desired application conditions of the target applications, using TreadStone's baseline gold dots technology on stainless steel substrate.

- *200W and 2 KW stack development and Demonstration*

Due to the budget limitation of the project, it was not affordable to design and make special stamping dies for the 200W and 2KW stack. Therefore, we used the rolled corrugated stainless foil with the straight channels for the demonstration of this project. Figure 19 shows the picture of the small plate with the rolled straight channels with gaskets.

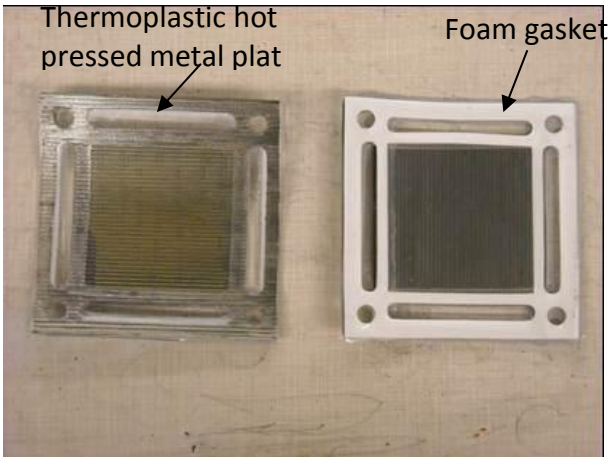

Figure 19. Pictures of the corrugated metal plate with laminated thermoplastic gasket and form gasket

Before the assembly of the full size stack, the flow field and the stack components and assembly process were evaluated using two-cell stacks with Gore PRIMEA Series 5561 MEA, (25μm membrane, 0.45mg Pt alloy cathode, 0.4mg Pt anode, Lot 00871619, PN P-03396). The active areas were 30cm^2 and 263 cm^2 for two-cell small stack and the other large two-cell stack, respectively. In comparison, another two-cell stack using machined POCO graphite plates was also assembled and tested under same condition of metal plate stacks. Their performances were compared to evaluate the flow field of the rolled corrugated plates.

Figure 20 shows the performance comparison of the two-cell stacks using Treadstone's metal plates and POCO graphite plates, tested at 65°C using fully humidified hydrogen and air. It shows that stack using TreadStone' metal plates had smaller internal ohmic resistance (120 mΩ.cm^2) than that of the stack with POCO graphite plates (157mΩ.cm^2), which led to the higher power density of the metal plate short stack than that of the POCO plate stack (solid lines in Figure 20).

After the plate flow field was verified using the two-cell stacks, the 300 W small stack (30 cm^2 active area of each cell) and 2KW large stack (263 cm^2 active area of each cell) were assembled and tested. Figure 21 shows the voltage distribution of the stack under OCV, 5A and 10A condition of the 300 W small stack. The voltages of each cell were fairly uniform, which indicated that the fuel and air flow distribution through each cell were uniform. Figure 22 shows the performance comparison of the small 200W stack with the small two-cell stack. It shows that the 300W stack had the same performance as the two-cell short tack.

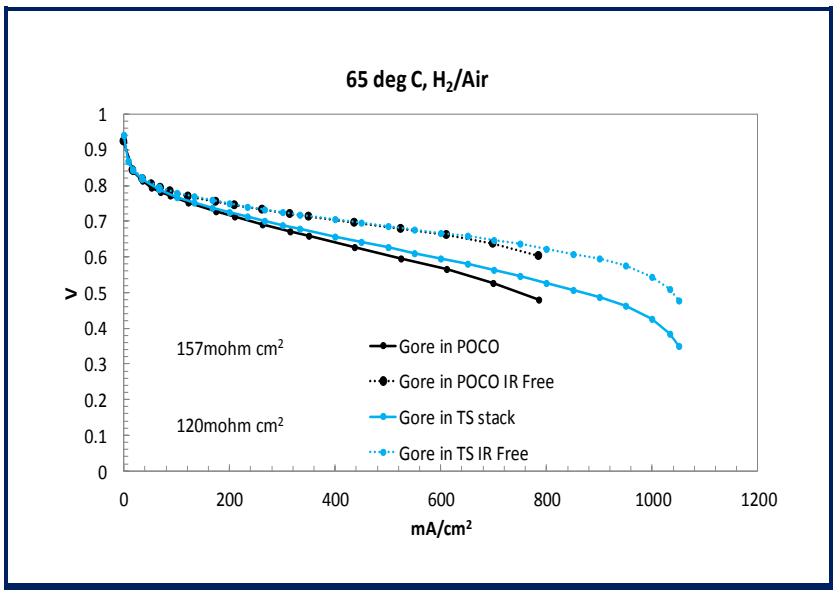

Figure 20. Performance comparison of 2-cell short stacks using TreadStone's metal plates, and POCO graphite plates.

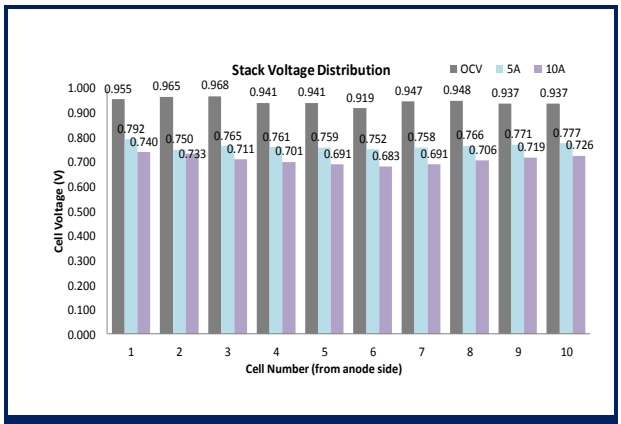

Figure 21. Cell voltage distribution for the 200 W stack at various output current

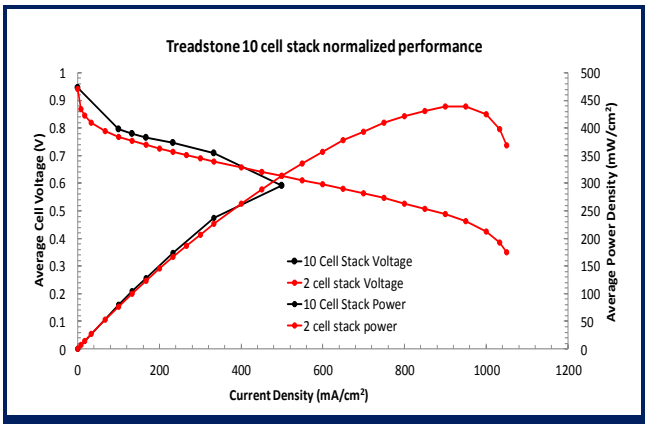

Figure 22. Compariosn of the average cell performance for the 300W stack and the two-cell short stack.

After the initial demonstration of the stack performance using TreadStone's metal plates, the long term durability tests of the stacks were carried out, but were not be able to finish. An issue with the fuel cell testing station led to the improper humidification of the membrane during the stack tests, which resulted to the damage of the membrane. The damage, eventually led to the rapid degradation of the stacks during the durability test.

- *Metal plate evaluations for automobile applications*

The demonstration of TreadStone's baseline metal plate for automobile applications was supported by Ford Motor Companies. The plate surface treatment was applied after the plates were stamped with Ford's standard flow field design, and welded to form the bipolar plate. The stack was tested at Ford's facility with their DJR dynamic operation testing protocols.

Before the official *in-situ* stack durability tests, Ford verified the properties of TreadStone's metal plates through *ex-situ* experiments. The results are summarized in Figure 23. In addition to the standard tests summarized in Figure 23, Ford conducted a more aggressive corrosion test defined for their stack operation conditions. The purpose of the test was to evaluate the robustness of the metal plates after short time high voltage exposure, which might occur during stack start and shut down processes. The test method was to compare the Cyclic Voltammetry (CV) curves of metal plates before and after the high voltage polarization treatments (6 hours under 1.6V_{NHE} with air purge and 0.5V_{NHE} with hydrogen purge). It was found the properties of TreadStone's plates met Ford's requirement.

Attribute	Metric	Unit	2015 DOE Target	Ford Data on Au-Dots
Corrosion anode	**Current density at active peak in CV**	μA/cm^2	<1	No active peak
Corrosion cathode	**Current density at 0.8 V_{NHE} in potentiostatic expt.**	μA/cm^2	<1	~0.1
Area Specific Resistance	**ASR (measured through plane) at 6 bar contact pressure** (includes both side surface; doesn't include carbon paper contribution)	mOhm.cm^2	<20	8.70 (as-recd flat samples)
Electrical Conductivity	**In-plane electrical conductivity (4-point probe)**	S/cm	>100	34 kS/cm
Formability	**% elongation** **(ASTM E8M-01)**	%	>40%	53(|| to RD*)/ 64 (⊥ to RD)
Weight	**Weight per unit net power** (80 kWnet system)	Kg/kW	<0.4	<0.30

Figure 23. Ex-situ evaluation data TreadStone's SS plates at Ford Motor. TreadStone's SS plates meet Ford's requirements.

Then, a 10-cell short, full size (300cm^2 active area) 2.5 kW stack was assembled and tested at Ford, using their DJR dynamic testing protocol. Figure 24 shows the picture of the stack in the testing stack. The durability test was continued for 1000 hours.

After the 1000 hours test, the stack was dissembled for the TPV (through plate voltage drop) measurement of all metal plates after the durability test, and visual inspection of any possible damages. Figure 25 shows the comparison of the stack performance before and after the 1000 hours durability test. The stack performance had slightly degradation, mainly due to the MEA degradation. Figure 26 shows the TPV (at 1A/cm^2) before and after the 1000 hours durability test. The initial TPV was 15 mV. After 1000 hours test, the TPV had ~2 mV increase. The chemical composition analysis of the condensed water from anode, cathode and coolant indicated that the metal ion content was below the limit of the analyzer (~ppb).

Figure 24. Picture of Ford's 10-cell short stack using TreadStone's SS plate technology

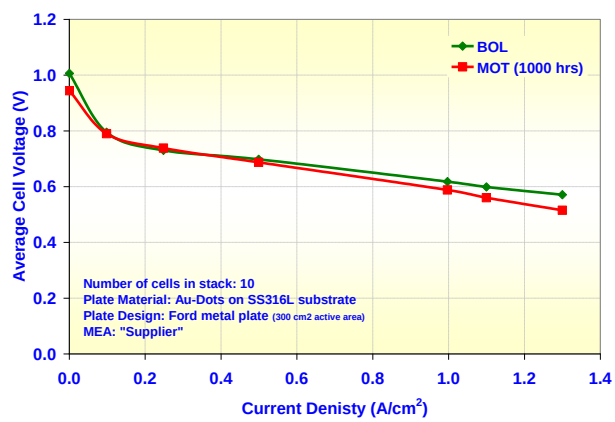

Figure 25. Initial and after 1000 hours operation performance comparison of the 10-cell stack

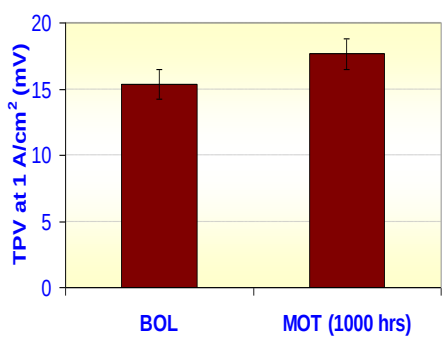

Figure 26. Comparison of the TPV before and after 1000 hours tests

After the first 10-cell stack test, Ford decided to test another 20-cell, 5 kW stack with the metal bipolar plates produced using TreadStone's optimized processing technique. These plates have more uniform contact resistance across the plate and between all plates (shown in Table 5). In order to mitigate the risk of the plate resistance increase during the lifetime test, Ford adjusted requirement of the initial (beginning of life, BOL) bipolar plate TPV to <10 mV at 1A/cm^2 current density. The objective was to ensure the plate TPV at the end of life (EOL, 5,000 hours) still below 20 mV. The stack used MEAs from W. L. Gore. During the durability test, the test was paused every 500 hours to remove one plate from the stack for TPV measurement and inspection. Table 7 summarizes the TPV of these plates at the beginning of life (BOL) and the

middle of life (MOL). It shows that there was no TPV increase on all plates during the 2000 hours test. Actually, the plate resistance was reduced after the durability. The reason for the TPV reduction could be that gold splats were slowly pressed flatter, under the high compression force of the assembled stack, which would increase actual area coverage of gold splats on plate surface, resulting in the lower electrical contact resistance and TPV.

Table 7. Comparison of plates TPV at beginning of life (BOL) and middle of life (MOL)

Plate #		**#18**	**#19**	**#17**	**#16**
Testing Time (hrs.)		**500**	**1000**	**1500**	**2000**
TPV (mV)	**BOL**	9.09	8.49	7.42	8.12
	MOL	5.90	7.21	5.93	5.67

The comparison of the stack performance before (BOL) and during the 2000 hrs is shown in Figure 27. It shows that there was slight performance degradation through the durability test. This performance degradation was due to the MEA degradation, instead of metal plates, because of the stable and low plate resistance during the 2000 hours test. This durability test demonstrated the stable performance of TreadStone's metal plate for PEM fuel cell applications.

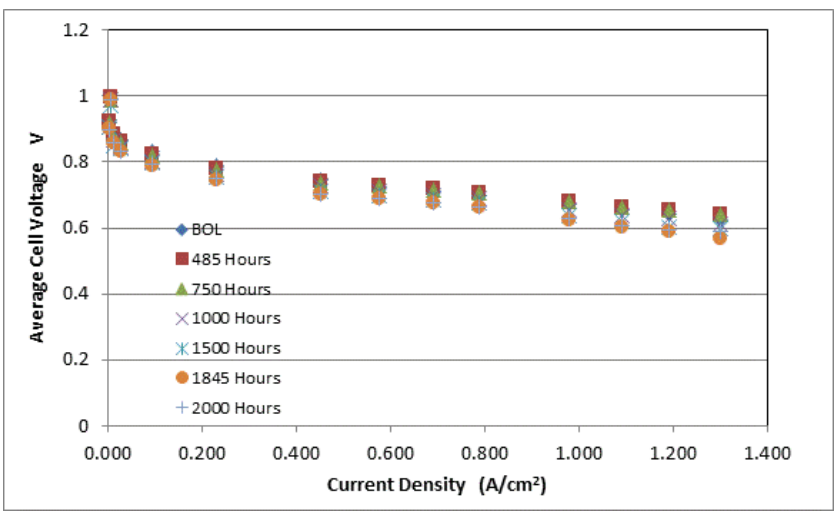

Figure 27: Performance comparison of the 20-cell stack using TreadStone's metal plates before (BOL) and during the 2000 hours durability test.

3. Product Developed under This Award

- *Publications*

i. Lin Zhang, Joshua Finch, Gerald Gontarz, Conghua Wang, "Development of low cost PEMFC metal bipolar plate", in ESC Transactions Vol. 33, "Polymer Electrolyte Fuel Cells 10" No. 1, p. 904, Oct. 2010

ii. Lin Zhang, Gerald Gontarz, Conghua Wang, "Development of low cost PEMFC metal bipolar plate", presentation in Fuel Cell Seminar, Nov. 2011, Orlando, FL

- *Network and collaborations*

The project has enhanced our market development efforts with foreign automobile companies. We have been in discussion with several clients for the application of this technology in their fuel cell stacks.

- *Other Products.*

This project has enable the application of the corrosion resistant technology in PEM electrolyzers and some flow battery systems, which leads to the corrosion resistant metal plate production and sale into these markets.

4. Acknowledgments

The author appreciates the support of the DOE EERE Fuel Cell Team. They not only provided the financial support for this project, but also the networking support with industrial partners, which is very important for the commercialization of the technology. The guidance from Fuel Cell Tech Team of USCAR (United State Council for Automobile Research) was also very valuable to the technology development. It helps the better alignment of the technology development toward what industry is focused on.

Our team partners have provided great contributions to this project. Dr. Shinichi Hirano, Mr. Mark Ricketts and George Solako have led the metal plate demonstration in automobile stacks at Ford Motor Company. Dr. Chinbay Fan led the portable and stationary stack development at Gas Technology Institute. Prof. Sanjay Sampath, Dr. Yang Tan and Dr. Yikai Chan from Stony Brook University have contributed in the thermal spray process characterization and optimization. Dr. Dane Wilson of Oak Ridge National Laboratory provided valuable support to the corrosion mechanism investigation. Mr. Anthony Mascarin of IBIS Associates led the production cost analysis. This analysis was very helpful in the fabrication technology selections for the low cost metal plate development.

The author also wishes to acknowledge the assistance from his colleagues at TreadStone, in particular Dr. Joshua Finch, Dr. Lin Zhang, Mr. Gerald Gontarz and Mr. Gerald DeCuollo.